

Signal Strength Based Indoor and Outdoor Localization Scheme in Zigbee Sensor Networks

Wen-Hsing Kuo, Yung-Sheng Chen, Kui-Tai Cheng, and Tai-Wei Lu

Abstract—Positioning schemes in sensor networks are presented in this study. A framework monitoring the signal strength based on the transmission protocol AODV and the placement of Zigees is established and used in sensor node positioning. To treat indoor and outdoor environments, two positioning schemes are presented accordingly. The indoor scheme clusters the localization zone into several subzones based on the strongest received signal, whereas the outdoor scheme adopts the estimated distance to determine the most possible position of the sensed node. Unlike existing studies, our methods do not need any location fingerprinting process in advance or location database. One-floor and multi-floor environment for indoor positioning cases are examined, where the accuracies of different node placements are studied. Two positioning algorithms used in outdoor cases are investigated, where field tests are conducted to evaluate the performance. Results show that the proposed methods can achieve good accuracy in both indoor and outdoor environments.

Index Terms—localization, positioning, sensor networks, signal strength, Zigbee.

I. INTRODUCTION

In the past decade, wireless sensor networks (WSNs) [1] [2] [3] [4] [5] are widely studied and developed. A wireless sensor network is composed of a distributed collection of sensor nodes with limited capability. By operating cooperatively of each node, different applications such as environmental monitoring, military surveillance, search-and-rescue operations, medical care and so on can be achieved. Among different physical standards of sensor networks, Zigbee [6] which bases on the IEEE 802.15.4 standard is one of the most potential technologies. Zigbee refers to a suite of communication protocols. As shown in Fig. 1, its PHY layer and MAC layer which are responsible for radio transmission and PAN (Personal Area Network) association/disassociation respectively are defined by IEEE 802.15.4 standard. On the other hand, the Zigbee Alliance defines the AP layer and NWK layer that control/manage objects, and decides the network topology respectively. Zigbee aims to form a low data rate network that

requires less cost and lower power consumption. Compared with other similar standards such as Bluetooth, each single device tends to require lower complexity and cost.

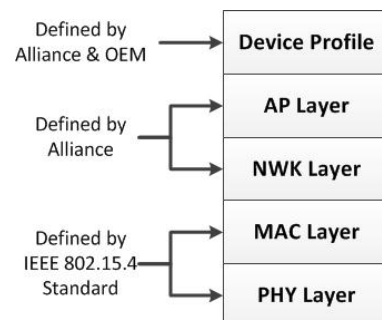


Fig. 1. Structure of Zigbee protocol.

According to the design of Zigbee, the supported topology can be mainly categorized as three types, i.e. star, cluster tree and mesh, as depicted in Fig. 2. In a star topology, there is only one coordinator which can manage the end devices. To extend the coverage and improve the maximum hop number of the network, the cluster tree topology allows Zigbee Routers to relay information between End Devices and the coordinator. To further extend the flexibility of the topology, the mesh networks allow multi-hop relaying between routers.

Localization has become a hot topic in sensor networks. Typical Global Positioning System (GPS) technology [7][8] pinpoints the receiving nodes based on the time latency of signals transmitted from different satellites, and yields typically 10m positioning error. On the other hand, the sensor network can also position the receiving node by detecting the signal strength of nodes from sensors whose locations are already known. Unlike GPS which provides global positioning, the sensing area of the sensor network is limited in its coverage. However, in the positioning aspects, it also has advantages over GPS. For example, it makes indoor positioning possible, and yields higher accuracy which GPS fails to achieve such as the work by Fang et al [5].

There are many different approaches of positioning in sensor networks. Some of them determine the distance to the node based on the time of arrival (TOA) of the transmission. To achieve this, the clocks of the receiver and the transmitter have to be synchronized, and the time difference between transmission and reception should be measured. [9] is a good example of these types of works. However, these kinds of methods need high accuracy of clocking and dedicated

Manuscript received February 16, 2014.

Wen-Hsing Kuo is with the Department of Electrical Engineering, Yuan Ze University, Chungli 320, Taiwan, ROC. (email: whkuo@saturn.yzu.edu.tw).

Yung-Sheng Chen is with the Department of Electrical Engineering, Yuan Ze University, Chungli 320, Taiwan, ROC. (corresponding author. phone: 886-3-4638800; fax: 886-3-4639355; e-mail: eeyschen@saturn.yzu.edu.tw).

Kui-Tai Cheng and Tai-Wei Lu are with the Department of Electrical Engineering, Yuan Ze University, Chungli 320, Taiwan, ROC.

synchronization mechanism. Therefore, they are not suitable for sensor networks which have nodes too numerous to synchronize. In addition, each node in a sensor network has lower complexity and thus less accurate clock.

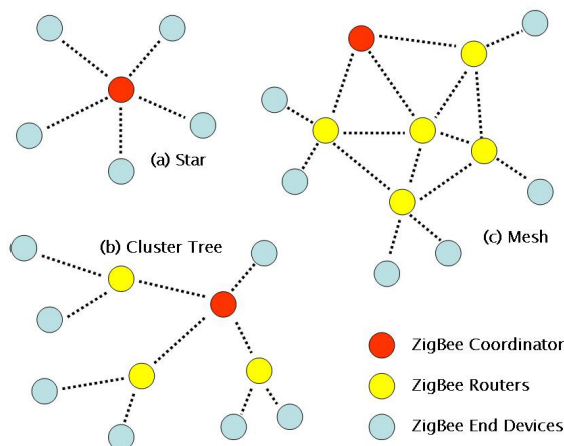


Fig. 2. Three topologies of Zigbee Networks.

Given above reasons, most positioning studies in sensor networks determine the location of nodes based on the Received Signal Strength Indication (RSSI) of the signal detected with nodes having known locations. Since nodes in different locations give different receiving patterns of signal strength, many works, such as [10] and [11], compare the received RSSI in a database which is built beforehand. This kind of system has to measure the received RSSI patterns first and store them into the database. During the positioning process, it compares the current measured one with the stored ones in the database to find the closest match. However, before the on-line phase, this kind of approach requires to collect location patterns all over the sensing area, which may be extremely time-consuming. For a sensor network having large coverage, it may even be infeasible. Designing a positioning algorithm based on the RSSIs is another approach. With a mathematical model, the position of nodes can be estimated by analyzing the RSSI signals. With this approach, the fingerprinting process is not necessary. Typically, the trilateration approach [12] is used in this kind of problems. While [13] studies the positioning performance under different path-loss conditions. This kind of works, however, can only be applied at open spaces since the signal strength may be affected by obstacles such as walls and doors, which are not considered by the algorithms.

In this work, we introduce the operational detail of Zigbee, and show how we modify the existing technologies to gather the received strength of signals. Then, two categories of localization algorithms are proposed, which are designed for indoor and outdoor positioning of sensor networks. Based on the RSSI of the signal, these algorithms can locate the position of the sensed node. The proposed approach does not need fingerprinting process and pattern database, thus a localization of sensor network can be conducted in a feasible and efficient way.

The remainder of this paper is structured as follows. In section II, we first introduce the system architecture and then detail the two proposed approaches. In section III, the implementation details and experimental results are presented

and discussed. Finally, the paper is concluded in section IV.

II. INDOOR AND OUTDOOR LOCALIZATION SCHEMES

A. System Architecture

In both indoor and outdoor environments, a common architecture gathering the information of the signal strength is needed. As illustrated in Fig. 3, the cluster tree topology is adopted in our proposed positioning framework as shown in Fig. 2(b), where several router nodes which positions have been known are placed into the environment as the positioning anchor. We call these router “sensing nodes” hereafter because they are responsible for detecting the Signal Strength of the received signal. When a certain node whose position is to be detected (called “sensed node” hereafter) appear in the network, all sensing nodes are used to measure the signal strength of the links, then report the data to the coordinator node which controls the network. The coordinator reports all gathered information to the PC in its back end, where the analytic algorithm and the localization process are performed there.

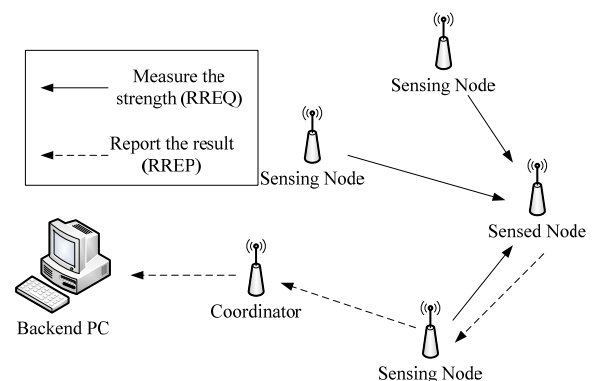


Fig. 3. System architecture.

According to the physical design of Zigbee, when a sensed node joins the network, it must negotiate with the coordinator and acquire a unique ID. After the initialization process, all other nodes in the network are informed with this new-coming node. Next, to report the signal strength as mentioned above, we modify the existing AODV (Ad hoc On-Demand Distance Vector) routing protocol, which is designed for enabling the transmission between two mobile nodes in an ad-hoc network. When initiating the connection, the source in AODV protocol sends Route REQuest (RREQ) packet in a flooding approach to find the destination, after receiving RREQ packets from different paths, the destination transmits Route REPLY (RREP) along the route it determines. We modify the protocol and implement the system as follows. When the coordinator starts to position this node, it transmits a modified RREQ packet containing a positioning FLAG (called P-RREQ). Then, the sensed node measures the signal strength from different sensing nodes where the P-RREQ is forwarded from, and includes the measured data into the modified RREP packet (P-RREP) while returning to the coordinator. Having gathered the signal strength from all reference nodes, the coordinator can provide them to

the backend PC for analysis.

Next we introduce the detail how the signal strengths from sensing nodes are measured. There is an information field called LQI (Link Quality Index) in the transmitted packet, which uses 8 bytes to represent the link quality (i.e. signal strength). When receiving the message from a node, the strength of the receiving signal is provided by the physical layer of the device and written in the field. Typically, the representation of LQI is different according to the device vendor. Before analyzing the strength of signals, the value of the LQI must be transferred into dB. Then, the system in the back end can use different positioning scheme to obtain the localization result.

B. Indoor Positioning Method

The positioning methods which base on the received signal strength acquired from the coordinator are detailed. In the indoor environment, the signal strength of the receiving signal may be severely affected by the intermediate barrier, such as doors and walls. Therefore, the receiving strength can effectively reflect the position only when there are no barriers between the sensing nodes and the analyzed node. Based on the structure of the building, our indoor positioning method places the sensing node in the ends of the corridor so that no matter where the position of the node is, at least two sensing nodes can directly receive the signal and provide useful information. Consider a building with four corridors, four sensing nodes can be placed in each end of the corridors as illustrated in Fig. 4.

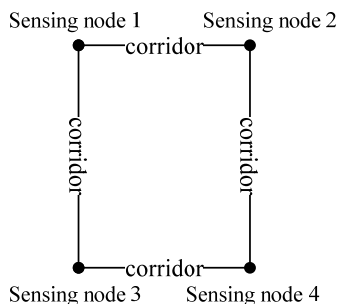


Fig. 4. An example of the node placement.

To determine the position of the node, three schemes are developed. Since the received strength of non-light-of-sight signals is weak and unstable, our indoor positioning schemes only use the strength of the line-of-sight signals. First the positioning plane can be divided into several zones according to the position of the sensing nodes. The algorithm localizes the sensed node within the zone based on the strongest signal strength. Next, to improve the accuracy, the positioning zone can be further divided into more sub-zones according to the second directly sensing node (i.e. the sensing node with the second strongest strength). To improve the correctness even further, the third scheme considers the proportion between the strongest and the second one in each sub-zone. When the former is much stronger than the latter, the node must be located near to this sensing node. On the other hand, if the receiving strengths between the two nodes are approximate, the node must be close

to the boundary of the zone. Fig. 5 illustrates the positioning zones of the three schemes.

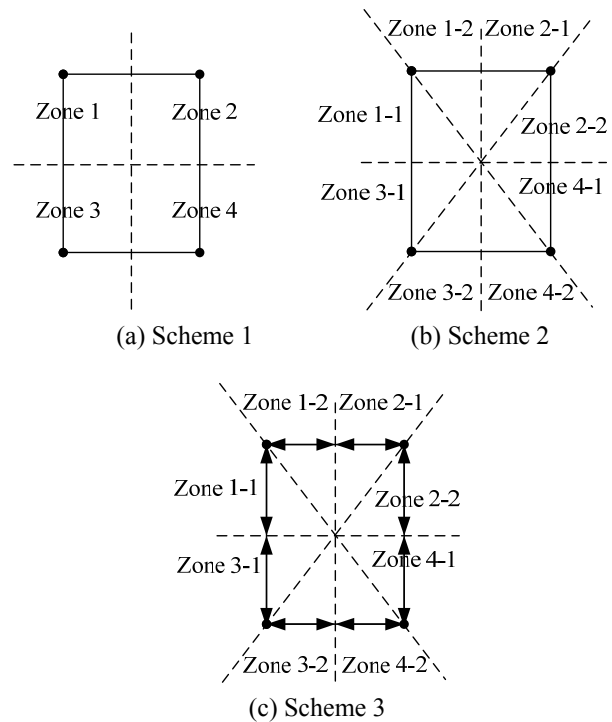


Fig. 5. Three positioning schemes in indoor environment.

The readers should be reminded that given the basic concept of the three indoor localization schemes, the actual implementation may be slightly different to the theoretical ones due to the physical layout of the building or the radio constraints of the devices.

C. Outdoor Positioning Method

In the outdoor environment, the positioning node can be put at anywhere in the positioning range instead of only in the corridor. However, compared to the indoor environment, there are fewer reflectors and obstacles, thus the strength of the receiving signal is mostly affected by the fading effect caused by the transmission distance. Accordingly we can measure the fading condition (i.e. the relationship between the receiving strength and the distance) in advance and use it to find the position of the node.

The signal propagation model in [14] is adopted in this study. This model describes the relationship between the signal strength and the transmission distance in an open area as $-10n \log_{10}d + A$, where n is a propagation constant, d is the transmission distance, and A is the received strength where the transmission distance is counted with one unit of the distance (e.g. one meter). By means of this model, we can first measure the receiving strength in different distances, and then adjust the value of n to let the model fit with the actual data. With this model, given the signal strength, the transmission distance can be found. Next, knowing the distance from each sensing node, the two following algorithms are used to pinpoint the positions of the sensed node, which are Circle Intersection Algorithm (CIA) and Line Intersection Algorithm (LIA) respectively. Let each sensing node draw a circle whose radius is the estimated

distance. CIA averages the locations of all the intersection points and makes it the position as shown in Fig. 6(a). Next let LIA draw the intersection lines between each two circles as illustrated in Fig. 6(b). Then, the intersection points of these lines are averaged. The performance of the two outdoor positioning schemes will be investigated in next section.

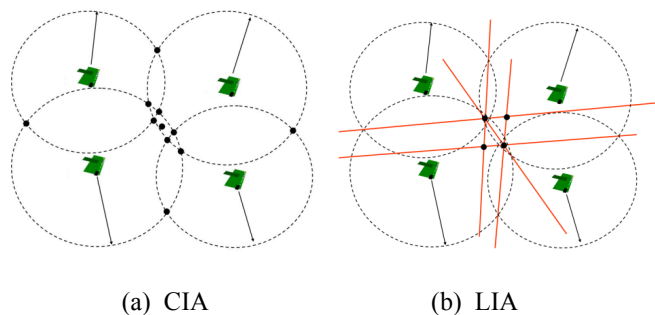


Fig. 6. Two positioning algorithms in outdoor environment.

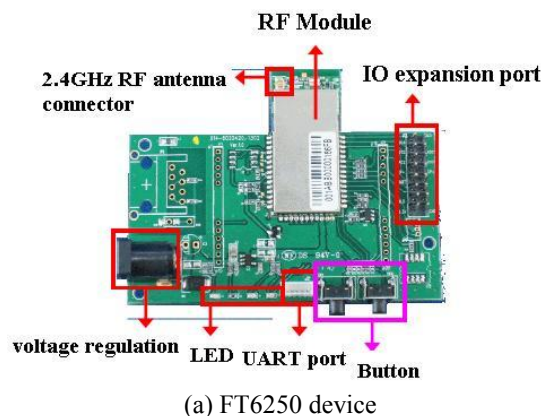
III. RESULTS AND DISCUSSIONS

A. Experimental Configuration

In the experiment, we use Zigbee devices FT6250 and FT6251 provided by FONTAL Technology [15]. Such a device is shown in Fig. 7(a), while its specification is detailed in Fig. 7(b). The protocol of AODV is modified as mentioned in section II.A. Different sensor nodes can be positioned by transmitting P-RREQ messages of the coordinator.

B. Indoor Results

The indoor positioning experiments are conducted in the 6th floor of building 7 at Yuan Ze University (YZU). Two different placements and the corresponding results are shown in Fig. 8(a) and 8(b). For comparing the actual position to the sensed position, we move the sensed node to the door of each room and observe what area it is placed in by scheme 1. The cluster of the sensed position determined by scheme 1 is marked by the color of the sensing node. However, for positions which have same receiving strength from two sensing nodes, they are given two colors. As shown in Fig. 8(a), we find that under this placement of the sensing nodes, some positions are placed into wrong area. The rooms in the bottom are close to either SN1 or SN3. However, they are detected in area 2 since SN2 senses the strongest receiving strength. This is because the center of the building is hollow, which lets the signal can directly pass through. Although it takes longer to walk from SN2 to these rooms, their line-of-sight distance is shorter. To fix this problem, we adjust the position of sensing nodes and conduct another position test but still using scheme 1, and the results are shown in Fig. 8(b). By moving the position of SN2, the rooms in the bottom are not classified to area 2 anymore, and the building can be perfectly clustered into four areas. The difference between Fig. 8(a) and 8(b) shows that the position of the sensing nodes is critical and may severely affect the positioning accuracy.



(a) FT6250 device

Item	Specification	
Model Number	FT-6250, FT-6251	
Network Standard	IEEE 802.15.4	
Data Rate	250kb/s	
Frequency Band and Operating Channels	2.405GHz ~ 2.480GHz Channel 11 ~ 26	
Receive Sensitivity (Typical)	-88dBm	
Available Transmit Power	-16dBm ~ 14dBm	
Settings	6 steps of control	
Range	Indoor (open office environment)	Outdoor (open space)
	100 M	700M
Antenna Type	Omni Dipole Antenna with IPEX connector	
Processor	16MHz, 32-bits RISC	
RAM Size	96KB	
Flash Size	128KB	
I/O Ports - UART0	Baud-Rate: 4800, 9600, 19.2K, 38.4K, 76.8K, 115.2K	
I/O Ports - UART1	Baud-Rate: 4800, 9600, 19.2K, 38.4K, 76.8K, 115.2K	
I/O Ports - ADC	4 inputs 12-bits resolution	
I/O Ports - DAC	2 × 2 inputs 11-bits resolution	
I/O Ports - Comparator	0/5/10/20mV hysteresis level	
Sensor Range	Temperature reading range: 0 to 70°C Humidity reading range: 5 ~ 90%RH	
Buttons	Button 1, Button 2	
LEDs	Power LED: power-on indicator, green color Status LED1: Reserved, N/A Status LED2: green color Status LED3: green color	
Power Draw	1W maximum	
Dimensions (W×L×H)	FT-6200: 194mm × 136mm × 246 mm FT-6250: 61mm × 136mm × 234 mm FT-6251: 61mm × 136mm × 234 mm	
Housing	No	
Environmental	Storage temperature: -20 to 70°C Operating temperature: 0 to 70°C Operating humidity: 5 to 90% (non-condensing)	
RS-232 Cable	1.8M length, 9pin D-Sub M/F	
AC Adaptor	Input: 110V, 60Hz	
Battery Holder	1.5V AA Battery × 3	
Software Development	Windows XP	

(b) The specification

Fig. 7. The sensor node used in the experiment.

Next we study a two-floor scenario by placing sensing nodes in the 6th and the 7th floor of the building, as shown in Fig. 9(a) and 9(b). At this time, SN2 and SN4 are placed more distant to the coordinator to extend the coverage of the network. Similar to the former experiments, most points are detected by its nearest sensing nodes. The only mispositioning between two floors is that, the zone of the coordinator also includes the position right above. Similarly, this is because of its short physical distance.

nodes to point B of each floor, all positions can be detected correctly by the sensing node of the floor it belongs to, because the ceiling of each floor prevent the signal from propagating to other floors, as shown in Fig. 11(b). The results of two above experiments show that the proposed scheme can also be used on a multi-floor environment and provide correct localization most of the time if the sensing nodes are placed in a better position.

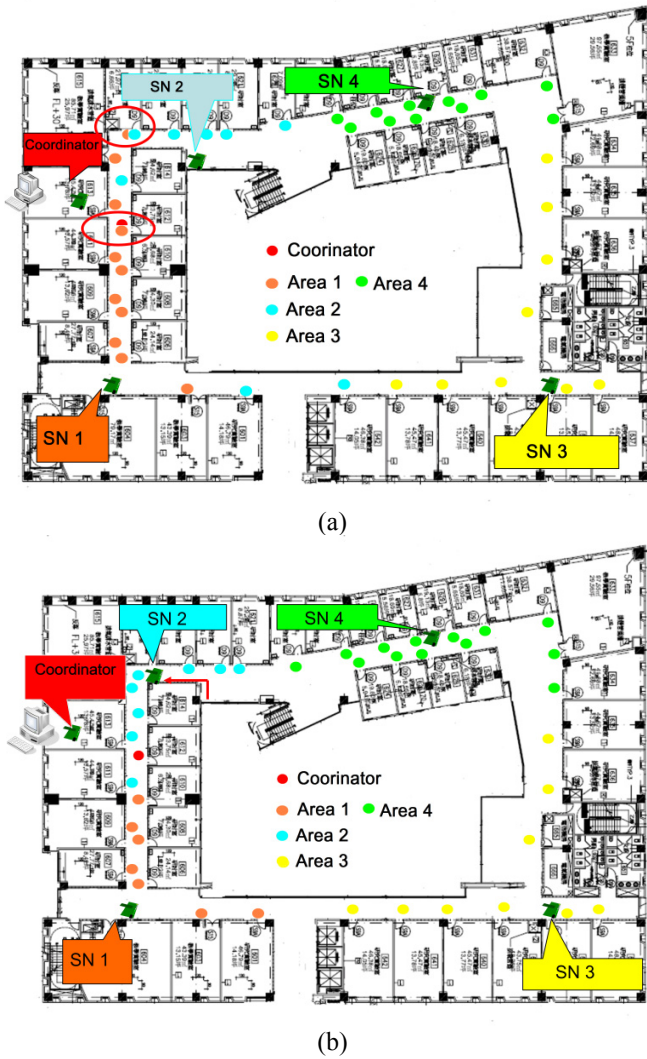


Fig. 8. Indoor results of different sensing positions.

Next we study a four-floor positioning by placing one sensing node on each of the 6th, 7th, 8th and 9th floor of the same building. As shown in Fig. 10, two different placements of the sensing nodes are used, which place a sensing one on each floor's position A and B respectively. Around each floor, we check if the sensing node on the same floor has the strongest received energy. The performance of position A is poor. Among all positions of the sensed nodes, the proportion of positioning the sensed node on the correct floor is 75%, 38%, 13% and 100% respectively. This is because the center of the building is a hollow open space, as shown in Fig. 11(a), thus the signal around the courtyard propagates between floors easily making the position less accurate. However, if we move the four sensing

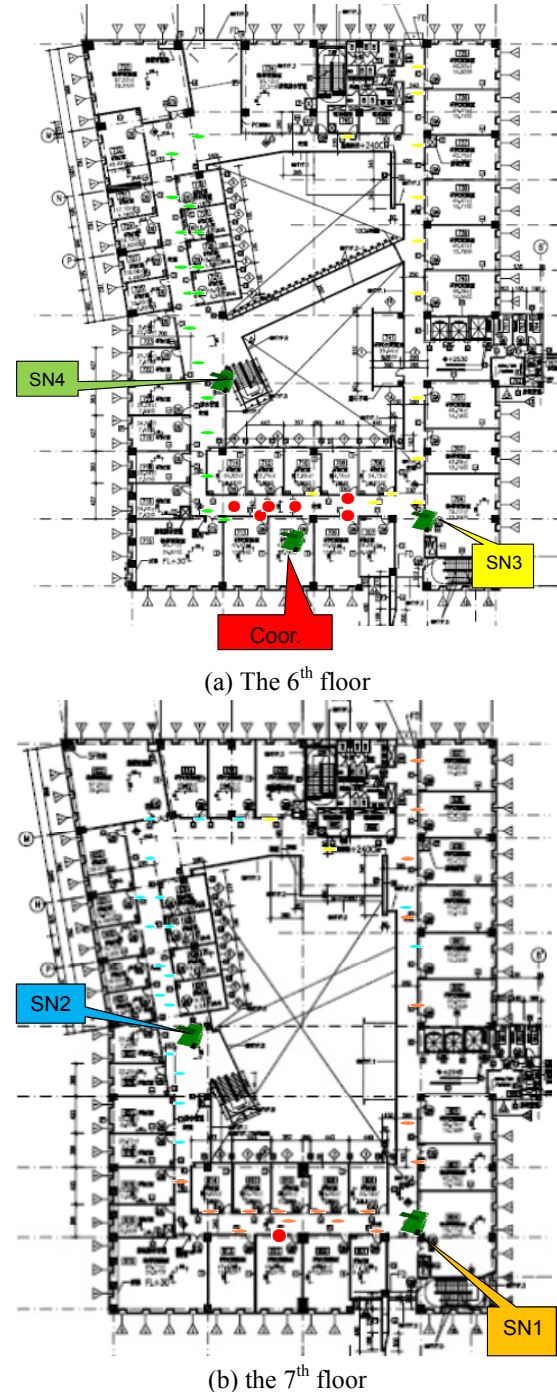


Fig. 9. Indoor results of a two-floor scenario.

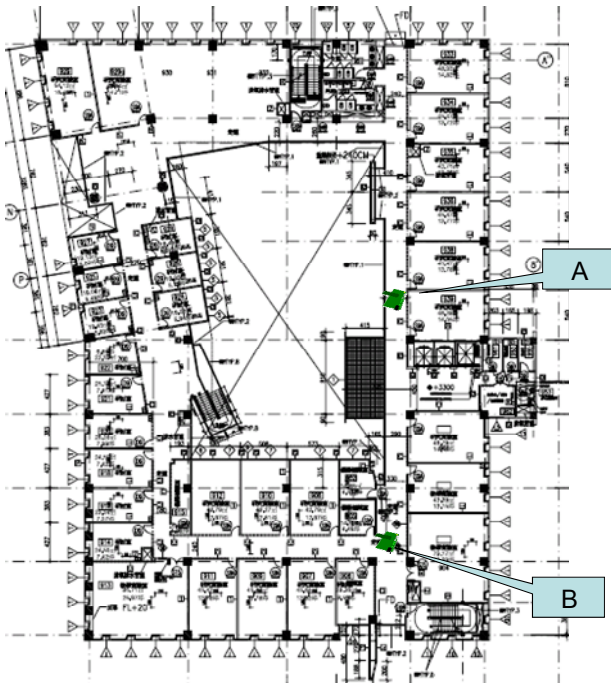


Fig. 10. Indoor results of a four-floor scenario.

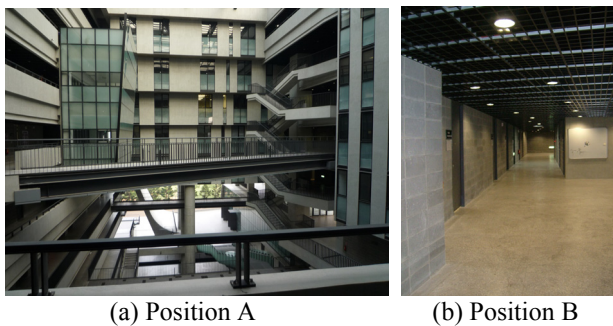
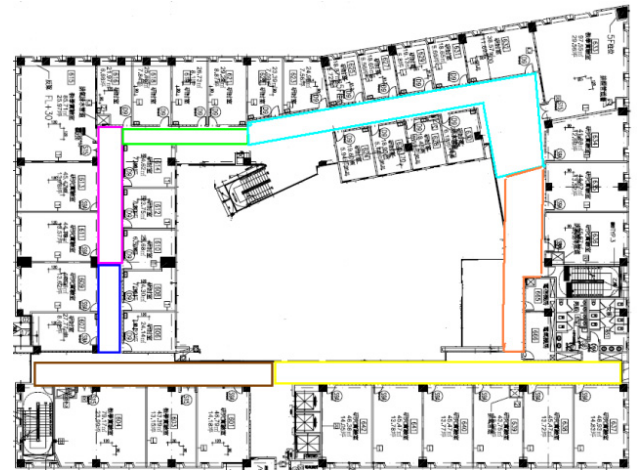


Fig. 11. The actual environment of position A and B.

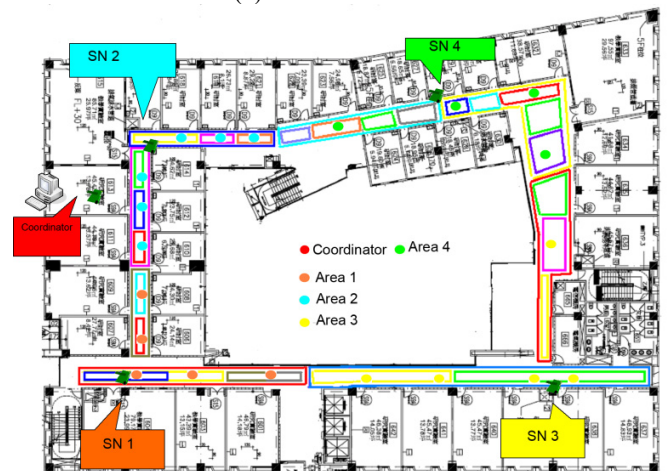
After studying the positioning in different floor, we investigate the scheme 2 which also considers the second strongest receiving strength, as shown in Fig. 12(a). Based on the same placement of Fig. 5, we can further divide each area into two sub-areas except for Area 4. The reason that Area 4 is not divided is that at most positions in the area, the second strongest node is SN 2 since the upper corridor is very narrow and can concentrate the radio signal. By means of the placement given in Fig. 8(b), we find that the algorithm of scheme 2 can correctly position the area of the node. The sensed positions can be estimated in the correct area.

Finally, as shown in Fig. 12(b), scheme 3 further divides each sub-area into three more areas based on the proportion of receiving strength between the strongest node and the second strongest one. We choose the number three based on the tradeoff between the size of the area and the successful positioning rate. When too more areas are divided into, it is more possible to be wrongly positioned. On the other hand, if the areas are too few, each area will be too big and thus the position cannot be

pinpointed. In our experiments, there is about 65% probability that the sensed node can be pinpointed in the correct area, while the probability of being positioned in the correct or adjacent areas are more than 95%. Considering the positioned area to the actual position, the positioning error is about 5m, which surpasses the average correctness of typical GPS technologies.



(a) Results of scheme 2.



(b) Results of scheme 3

Fig. 12. Indoor results of scheme 2 and 3.

C. Outdoor Results

Before conducting outdoor experiments, the relationship between the Received Signal Strength Indication (RSSI) and the distance must be studied. Comparing between the model and the actual measured data, we find that the trend between the two is very approximate. In addition, when $n=0.344$, the model approximates the actual measured results with minimal standard error. The difference between the analytical data and the actual results is shown in Fig. 13. However, when the distance to the sensed node is greater than 15m, the accuracy of the expected distance will decrease, which implies that to position the node more correctly, the maximal distance between the sensed node and the sensing nodes should be less than 15m.

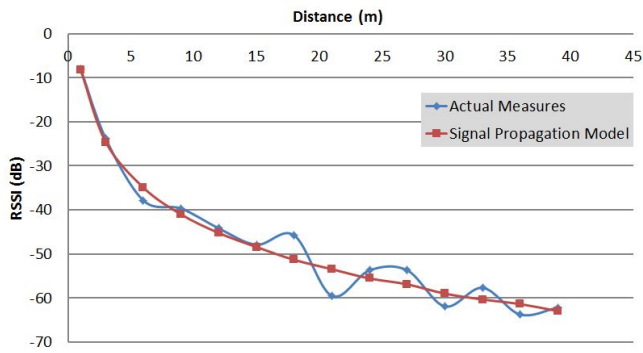


Fig. 13. The results of RSSI (dB) versus distance (m) with the signal propagation model in [14] and the actual measures.

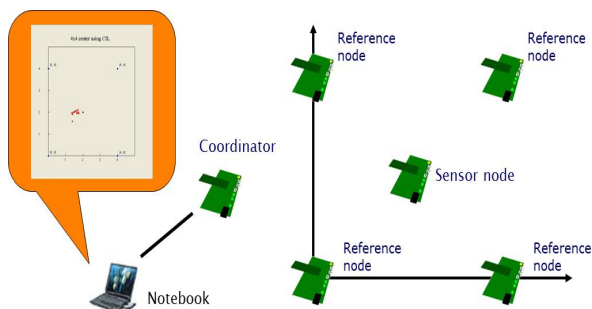


Fig. 14. Setup of our experiments.

D. Analysis of CIA and LIA algorithms

In this section, we conduct field tests to estimate the two outdoor positioning algorithms, namely CIA and LIA. A comprehensive experiment has been taken at a free space near building 7 hall at YZU. Once all nodes are placed, each run is performed until 100 estimations obtained, where the position of sensor node is estimated every 5 seconds. The experiments are divided into the following four parts:

Experiment 1. Place four reference nodes in square form and sensor node at center, then test the accuracy with different size of localization area.

Experiment 2. Place four reference nodes in square form and sensor node at corner, then test the accuracy with different size of localization area.

Experiment 3. Place four reference nodes into irregular forms, i.e. parallelogram, trapezoid and triangle, and then test their accuracies.

Experiment 4. Compare the accuracy between indoor and outdoor.

In experiment 1 of square form, the measures are performed by the experimental setup as illustrated in Fig. 14. In our experiments, we setup the reference-node layouts, e.g. $4m \times 4m$, $6m \times 6m$, $8m \times 8m$, and $10m \times 10m$ as shown; and use the localization algorithms, CIA and LIA, respectively to position the sensor node. The measures on each case are given in Fig. 15, where triangular and dotted marks represent the nodes and the

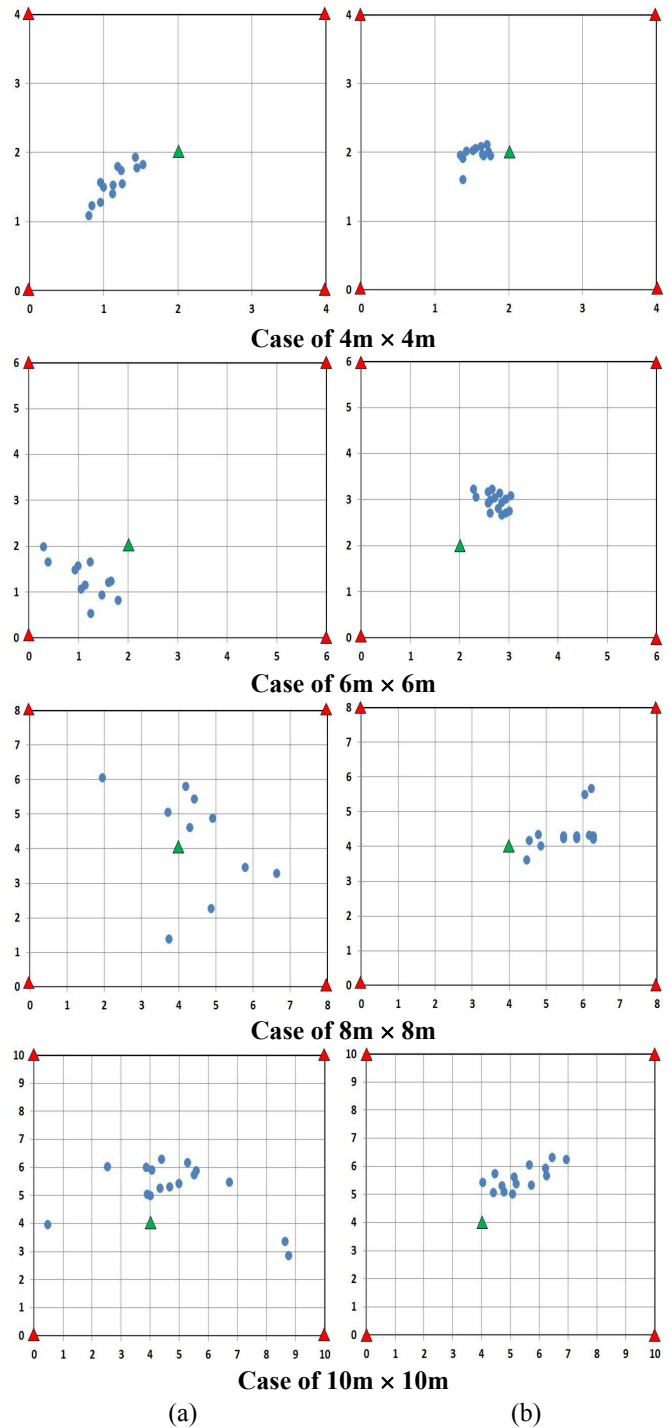


Fig. 15. Measured details by (a) CIA, and (b) LIA for the results given in Table 1. Here the sensor node is put at (2, 2), (2, 2), (4, 4), and (4,4) in the case of $4m \times 4m$, $6m \times 6m$, $8m \times 8m$, and $10m \times 10m$, respectively.

measured locations, respectively. The detailed statistics of position errors are given respectively in Fig. 16. The minimum, maximum, and average errors are reported in Table 1. In the $4m \times 4m$ square, the average error of LIA is only 36 cm and that of CIA is 89cm. In the $6m \times 6m$ square, the performance of both

algorithms is almost the same. In the larger squares, i.e. the 8m × 8m and 10m × 10m, LIA gains 1.68m and 1.94m average errors, whereas CIA gains 1.98m and 2.59m, respectively. It means that the localization accuracy of LIA is better and more concentrated than that of CIA.

In experiment 2, the layout of reference nodes is the same as that in experiment 1 but the sensor node is put at corners, i.e. (0, 1), (1, 5), (0, 1), and (0, 1) in the corresponding case. The measured details are shown in Fig. 17. This experiment shows that the accuracy of using CIA is not good, where its average error is almost greater than 3m. The average error of using LIA in the 4m × 4m and 6m × 6m is less than 1m and in the 8m × 8m and 10m × 10m is less than 2m. The accuracy of using CIA in corner and in center is almost the same. This further confirms that the performance of LIA is better than that of CIA.

Table 1. The minimum, maximum, and average errors for experiment 1.

Error(m)		Minimal error	Maximal error	Average error
Area (m ²) / Method				
4×4	CIA	0.33	1.82	0.89
	LIA	0.24	0.82	0.36
6×6	CIA	0.74	1.66	1.16
	LIA	0.93	1.39	1.12
8×8	CIA	0.89	3.40	1.98
	LIA	0.58	2.34	1.68
10×10	CIA	0.97	6.08	2.59
	LIA	0.32	3.46	1.94

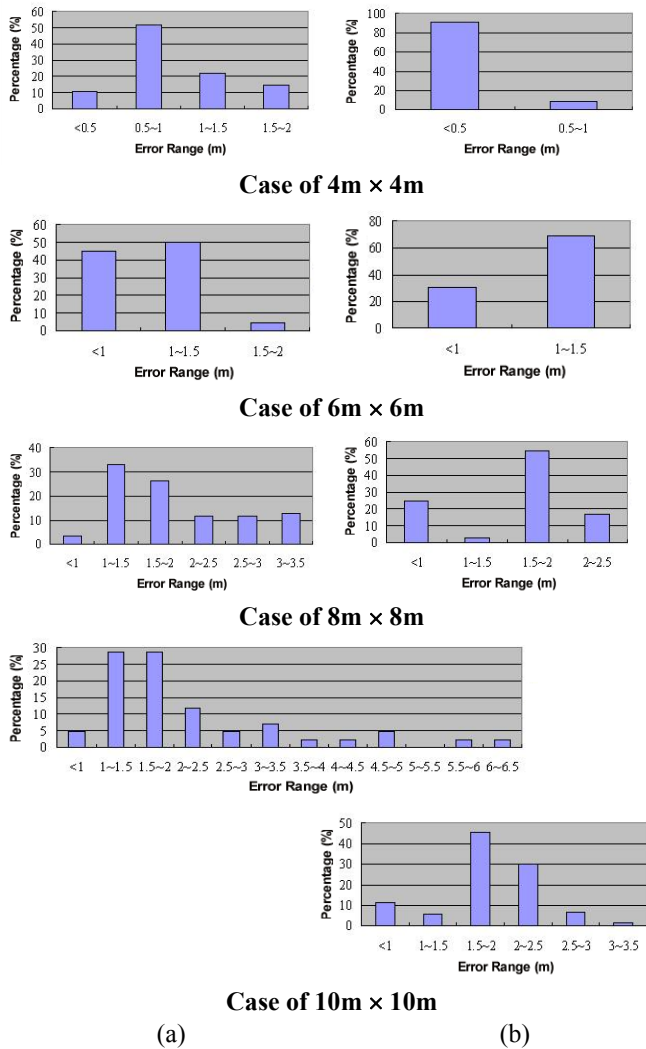


Fig. 16. Statistics of position errors for the results given in Fig. 15, by (a) CIA, and (b) LIA. Here the sensor node is put at (2, 2), (2, 2), (4, 4), and (4,4) in the case of 4m × 4m, 6m × 6m, 8m × 8m, and 10m × 10m, respectively.

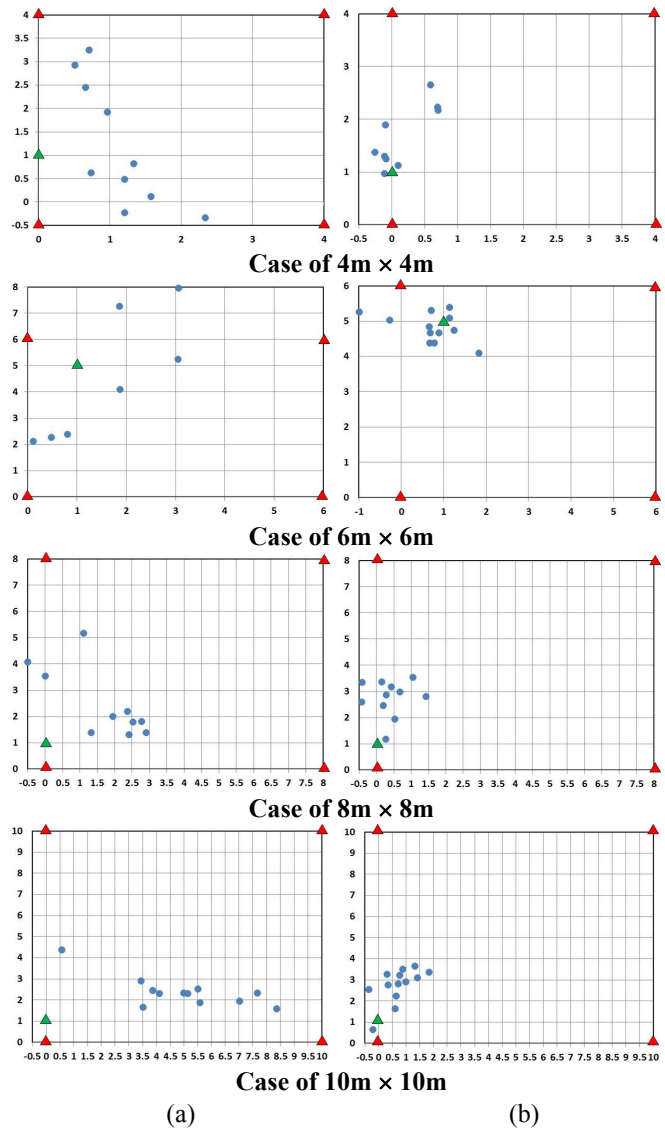


Fig. 17. Measured details by (a) CIA, and (b) LIA to investigate the influence of putting sensor nodes closing to the corner. Here the sensor node located at (0, 1), (1, 5), (0, 1), and (0, 1) are used respectively.

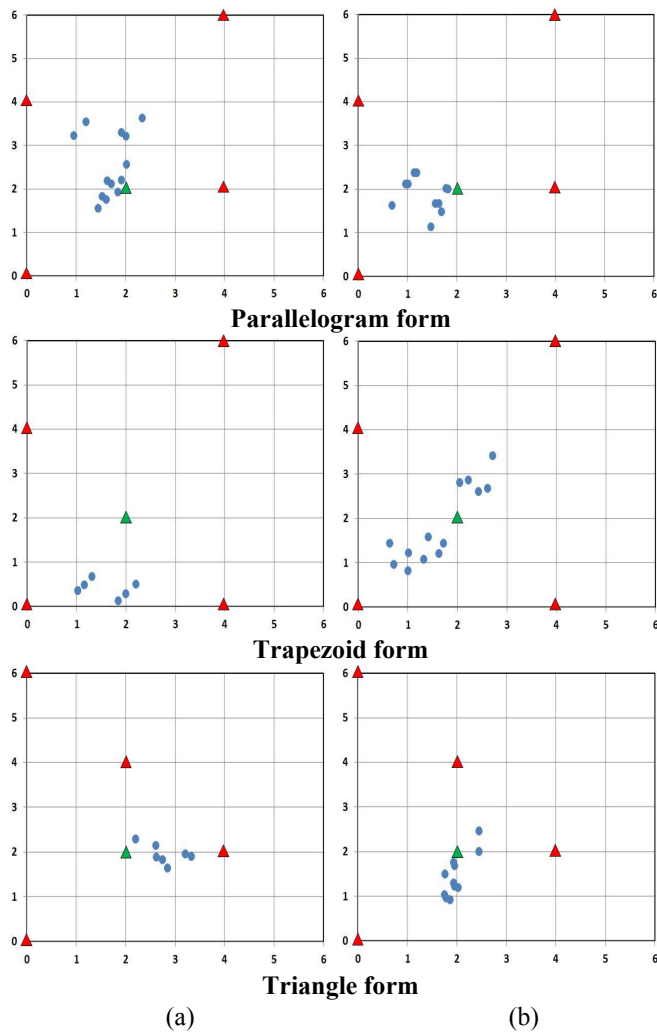


Fig. 18. Measured details by (a) CIA, and (b) LIA for parallelogram, trapezoid and triangle forms.

In experiment 3, four reference nodes placed into irregular area, i.e. parallelogram, trapezoid and triangle are further used to verify the proposed algorithms. In parallelogram form, four reference nodes are put at (0, 0) (0, 4) (4, 2) (4, 6). In trapezoid form, four reference nodes are put at (0, 0) (0, 4) (4, 0) (4, 6). In triangle form, four reference nodes are put at (0, 0) (0, 6) (2, 4) (4, 2). The sensor node is put at (2, 2) for measuring. The corresponding results are depicted in Fig. 18. The detailed statistics of position errors are given respectively in Fig. 19, and the minimum, maximum, and average errors are listed in Table 2. In this experiment of putting reference nodes in irregular form, the average error of using LIA is less than that of using CIA, which further confirms that the LIA is more accurate than CIA.

In experiment 4, four reference nodes placed in $4m \times 2m$ and $4m \times 4m$ rectangle are used to investigate the accuracy between indoor and outdoor, as well as their difference. Here the indoor experiment is held at Computer Vision Lab of Electrical Engineering Department, YZU. In $4m \times 2m$ case, four reference nodes are put at (0, 0) (0, 2) (4, 0) (4, 2), and the sensor node is

put at (2, 1) for measuring. In $4m \times 4m$ case, four reference nodes are put at (0, 0) (0, 4) (4, 0) (4, 4), and the sensor node is put at (2, 2) for measuring. The performance measures are listed respectively in Table 3(a) and 3(b). In the case of $4m \times 2m$, the accuracies of both CIA and LIA in the outdoors and indoors are not quite different, whereas in the case of $4m \times 4m$, the measuring accuracy in outdoor is better than that in indoor. Further the indoor positioning points are less concentrated, which is due to too much interferences like doors, walls and other obstacles in indoor environment and thus affecting the quality of reception. These comparisons show that the outdoor-aiming method can also be used in indoor scenario as long as there are no obstacles in the sensing area.

As a result, no matter CIA or LIA, the average positioning error is lower than 3 meters, which is much smaller than the typical GPS positioning error. The outdoor positioning scheme possesses better accuracy than the indoor positioning scheme since there are no obstacles between the sensed node and the sensing node for outdoor case, thus the receiving strength can provide more information to the localization algorithm.

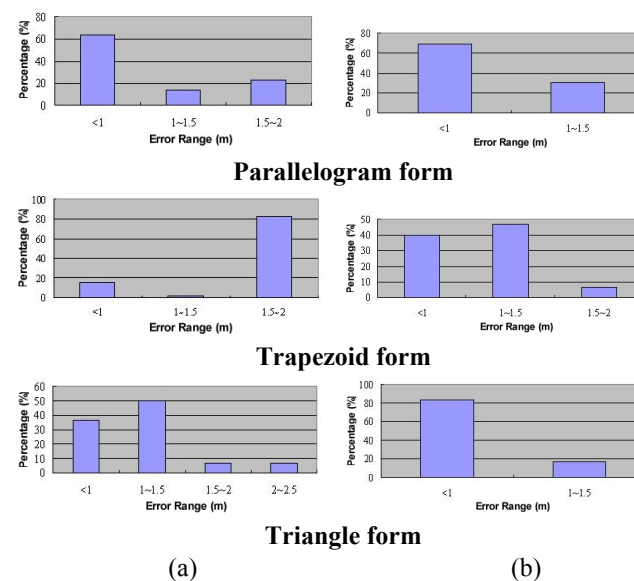


Fig. 19. Statistics of position errors for the results given in Fig. 18, by (a) CIA, and (b) LIA. Here the sensor node is put at (2, 2) in the parallelogram, trapezoid and triangle area, respectively.

IV. CONCLUSION

The signal strength based positioning methods in sensor networks have been studied in this paper. By modifying AODV protocol and utilizing the LQI in PHY layer of Zigbee sensor networks, the signal strength of a node can be measured by several sensing nodes and reported to the coordinator node. To perform the positioning process based on the received data, two approaches including indoor and outdoor cases are separately studied and discussed in this paper. Since these two methods do not require localization fingerprint process beforehand and the synchronization between nodes, they can provide a good

accuracy with low overhead from the viewpoint of the implementation cost. In indoor method, the receiving strength cannot be directly transformed into the distance since the obstacles conditions are quite different all over the building. Therefore, the building is clustered into many zones, and the position is determined by several nodes with the strongest receiving strength. On the other hand, signal strength is used to estimate the distance in outdoor method. Then, two approaches are presented to pinpoint the sensed node. Experiments are conducted to observe the accuracy of the proposed methods. Results show that our approaches can provide satisfying accuracy in both indoor and outdoor environment. By adjusting the position of the sensing node according to the layout of the building, the accuracy of indoor position can be improved. On the other hand, since the blocking effect of buildings does not exist in outdoor environment, the outdoor method provides even better accuracy. In the future, we will extend the research to more complicated environment such as 3-D positioning.

Table 2. The minimum, maximum, and average errors for experiment 3.

Error(m)		Minimal error	Maximal error	Average error
Area form / Method				
Parallelogram	CIA	0.17	2	0.86
	LIA	0.16	1.36	0.78
Trapezoid	CIA	0.48	1.89	1.57
	LIA	0.59	1.64	1.01
Triangle	CIA	0.29	2.37	0.99
	LIA	0.25	1.35	0.73

Table 3. Comparisons of CIA and LIA with indoor and outdoor situations, where (a) 4m × 2m and (b) 4m × 4m.

(a)

Error(m)		Minimal error	Maximal error	Average error
Area (m ²) / Method				
Indoor 4×2	CIA	0.1	1.18	0.57
	LIA	0.1	0.64	0.3
Outdoor 4×2	CIA	0.16	1.16	0.69
	LIA	0.16	1.1	0.38

(b)

Error(m)		Minimal error	Maximal error	Average error
Area (m ²) / Method				
Indoor 4×4	CIA	0.38	2.12	1.08
	LIA	0.36	1.86	0.77
Outdoor 4×4	CIA	0.33	1.82	0.89
	LIA	0.24	0.82	0.36

ACKNOWLEDGMENT

The authors are grateful to the referees; their thoughtful in-depth detailed comments have been very helpful in the revision of this article.

REFERENCES

- [1] J. Adams, "Designing with 802.15.4 and Zigbee," in *Proceedings of Industrial Wireless Applications Summit*, San Diego, CA, Mar. 2004.
- [2] I. F. Akyildiz, W. Su, Y. Sankarasubramaniam, and E. Cayirci, "A Survey on Sensor Networks," *IEEE Communications Magazine*, pp. 102-114, 2002.
- [3] N. Aslam, W. Phillips, and W. Robertson, "A Unified Clustering and Communication Protocol for Wireless Sensor Networks," *IAENG International Journal of Computer Science*, vol. 35, no. 3, pp. 249-258, 2008.
- [4] J. Han, C.-S. Choi, and I. Lee, "More efficient home energy management system based on ZigBee communication and infrared remote controls," *IEEE Transactions on Consumer Electronics*, vol. 57, pp. 85-89, 2011.
- [5] S.-H. Fang, C.-H. Wang, T.-Y. Huang, C.-H. Yang, and Y.-S. Chen, "An enhanced ZigBee indoor positioning system with an ensemble approach," *IEEE Communications Letters*, vol. 16, no. 4, pp. 564-567, 2012.
- [6] The ZigBee alliance website. <http://www.zigbee.org/>
- [7] B. Hofmann-Wellenhof, H. Lichtenegger, and J. Collins, *Global Positioning System: Theory and Practice*, New York: Springer-Verlag, 4th edition, 1997.
- [8] S Capkun, M Hamdi, and J- Hubaux, "GPS-free positioning in mobile ad-hoc networks," in *Proceedings of the 34th Annual Hawaii International Conference on System Sciences (HICSS '01)*, Maui, Hawaii, USA, pp. 3481-3490, 2001.
- [9] G. Balogh, A. Lédeczi, M. Maróti, and G. Simon, "Time of arrival data fusion for source localization," in *Proceedings of The WICON Workshop on Information Fusion and Dissemination in Wireless Sensor Networks (SensorFusion 2005)*, Budapest, Hungary, 2005.
- [10] K. Kaemarungsi, "Design of Indoor Positioning System Based on Location Fingerprint Technique," *Master's thesis*, University of Pittsburgh, USA, 2005.
- [11] K. Pahlavan, X. Li, and J. P. Makela, "Indoor geolocation science and technology," *IEEE Communications Magazine*, vol. 40, no. 2, pp. 112-118, 2002.
- [12] M. Srbnovska, C. Gavrovski, V. Dimcev, "Localization Estimation System Using Measurement of RSSI Based on ZigBee Standard," *ELECTRONICS*, Sozopol, Bulgaria, 2008.
- [13] X. Li, "RSS-Based Location Estimation with Unknown Pathloss Model," *IEEE Transactions on Wireless Communications*, vol. 5, no. 12, pp. 3626-3633, 2006.
- [14] K. Aamodt, "Chipcon Products from Texas Instruments," *Application Note AN042 (Rev. 1.0)*.
- [15] FONTAL Technology's High Power ZigBee Starter Kits (FT-6200) provide all the software tools and hardware required to get the first-hand experience with wireless sensor networks (WSN). <http://www.doctorsoft.com.tw/cetacean/front/bin/cglist.phtml?Category=127075>